In vivo targeted delivery of large payloads with an ultrasound clinical scanner

Olivier Couture[a)]
Institut Langevin, ESPCI, 10 rue Vauquelin, Paris 75005, France and CNRS, France

Alan Urban[b)]
Laboratoire de Neurobiologie, Optogenetics and Brain Imaging, ESPCI, 10 rue Vauquelin, Paris 75005, France and CNRS, France

Alice Bretagne[b)]
MMN, Gulliver, ESPCI, 10 rue Vauquelin, Paris, 75005, France

Lucie Martinez
Laboratoire de Neurobiologie, Optogenetics and Brain Imaging, ESPCI, 10 rue Vauquelin, Paris 75005, France and CNRS, France

Mickael Tanter
Institut Langevin, ESPCI, 10 rue Vauquelin, Paris 75005, France and INSERM, France

Patrick Tabeling
MMN, Gulliver, ESPCI, 10 rue Vauquelin, Paris 75005, France and CNRS, France

(Received 3 February 2012; revised 20 June 2012; accepted for publication 22 June 2012; published 1 August 2012)

Purpose: Performing drug-delivery with an ultrasonic imaging scanner *in situ* could drastically simplify treatment and improve its specificity. Our objective is to deliver large amounts of an encapsulated agent *in vivo* using a clinical ultrasound scanner with a millimetric resolution. This study describes the encapsulation of fluorescein within ultrasound-inducible composite droplets and its targeted release in predefined zones in the liver of rats.
Methods: An aqueous solution of fluorescein was encapsulated within perfluorocarbon liquid in 4 μm monodisperse droplets using a microfluidic system. The agent was then injected within the femoral vein of 12 rats. After exploratory ultrasound imaging, the sonographer defined five zones in the liver and a release sequence was initiated on the same apparatus. The surface of the liver was observed under fluorescence macroscopy and intraoperative fluorescence camera *in vivo*, before liver samples were sliced for pathology.
Results: Following the conversion of the droplets, a 25 dB increase in contrast was observed in the zones selected by the sonographer. These hyperechoic regions were colocalized with the bright fluorescent spots observed on the surface of the liver. A minimum peak-negative pressure of 2.6 MPa, which is within regulations for imaging pulses, was required for the delivery of the content of the droplets. The tissue and cellular structures were not affected by the exposure to the release sequence.
Conclusions: Since composite droplets can carry various therapeutic and imaging agents, they could deliver such agents specifically in any organ accessible to ultrasound. [http://dx.doi.org/10.1118/1.4736822]

Key words: ultrasound, surgery, multiple emulsion, microfluidics, marker, imaging technique, drug delivery

I. INTRODUCTION

Currently, tumor diagnosis and therapy are done separately. Cancer patients first undergo several imaging techniques exploiting different contrast mechanisms to describe the spatial distribution of their tumors. Then, a higher power modality, such as surgery, radiotherapy or localized heating, is performed to destroy or remove the diseased region. However, if imaging scanners were capable of delivering large amounts of agents, which could either stain, destroy or transfect tissue locally, both diagnostic and therapeutic could be combined. Following the design of versatile carrying agents sensitive to acoustic waves, ultrasound scanner could be transformed into handheld therapeutic devices. Treatment could hence be planned and induced by the same apparatus, leading to simplified procedures with a very high spatial resolution.

Ultrasound is already ubiquitous as a high-resolution imaging modality. It can penetrate up to 10 cm of human tissue, giving access to most internal organs, with a resolution in the submillimeter range. Modern ultrasound systems rely on electronic delays for tissue-scanning and can thus be made to focus acoustic waves anywhere within a plane. These advantages of spatial localization and penetration could also apply to therapeutic purposes since ultrasound can induce various bioeffects at higher pressures.[1] Acoustic waves act through several processes such as thermal deposition,[2]

cavitation induction,[3] sonoporation,[4] or blood-brain barrier disruption.[5] Heat generation and cavitation are already used clinically for therapeutic purposes, but they require large ultrasound sources, which are not adapted for imaging.

The bioeffects of ultrasound can be greatly enhanced by the introduction of acoustically sensitive agents.[6,7] For instance, microbubbles, which are classically used as contrast agents in acoustic imaging, can also affect surrounding tissue at pressures which are more typical of imaging applications. Due to their size, these microbubbles remain vascular, but still pass through capillaries. Their high compressibility and resonant behavior induce high amplitude oscillations which rapidly become nonlinear, helping their acoustic detection.[8] Violent oscillations can even lead to the disruption of their shell and the dissolution of their internal gas.

For neighboring cells, vibrating microbubbles can have drastic effects, such as opening pores on their membrane or induce leakage in the endothelial cells forming the blood brain barrier.[9–12] Because of their high sensitivity to ultrasound, microbubbles have been rapidly exploited for targeted drug delivery.[13] Drugs have been inserted in their lipidic shell, in polymer shells[14] and in liposomes loading.[15] DNA has also been combined to microbubbles and transfected on site.[16] Ultrasound combined to microbubbles could thus perform both an imaging and a therapeutic role concomitantly. However, the drug-carrying ability of microbubbles is limited to their surface, reducing the amount of agents being transported.

Nongaseous carriers have also been reported.[17–19] These agents, often temperature-sensitive nanoparticles, can be vaporized by the heat induced at the focus of powerful ultrasound sources. Other liquid droplets are rather converted by the localized drop in acoustic pressure, a fast process that can arise within 1 μs if the acoustic pressures are sufficiently large. These liquid particles exploit the small intermolecular binding force of low-boiling perfluorocarbon, such as perfluoropentane or perfluorohexane.[20] A significant advantage of these droplets, which can be smaller than the pore size in tumor vasculature, is that they can eventually penetrate the extravascular space in diseased tissue and serve as a precursor for an imaging agent. Moreover, liquid perfluorocarbon can be emulsified with lipid to carry large amount of lipophilic drugs[21] or agents can be modified with fluorine to be readily encapsulated in the droplets.[22] In general, most ultrasound-sensitive carriers are specialized into the confinement of lipophilic drugs. Many are plagued with the compromise between carrying capability, in the lipid phase, and acoustic pressure threshold for release, which depends on the perfluorocarbon fraction.

Recently, our team introduced composite droplets that can carry two-third of their volume in hydrophilic payload and can be released and monitored with a conventional ultrasonic scanner.[23–25] These droplets are water-in perfluorocarbon-in water double emulsion produced by microfluidics to prevent embolism. We believe that a wide variety of injectable agents could be added to the inner aqueous phase. Interestingly, the perflurocarbon creates a barrier between the internal aqueous phase and the surrounding fluid, which minimizes leakage of the content. Moreover, this thermodynamically unstable monodisperse construct has a sharp pressure threshold of release, which is within the regulatory guidelines for ultrasound imaging. Such sensitivity allows the drug release to be performed with the same ultrasound transducer and scanner as the one used during the diagnostic, allowing both steps to be performed in parallel. For safety considerations, this feature is a key advantage of our composite droplets for drug delivery as it ensures *de facto* a coregistration of the imaged region and the targeted release points. Indeed, the focused beams transmitted by the unique probe provides both the image information and the local drug release.

As a first application of these ultrasound-induced droplets, we proposed to tattoo deep tissue under radiological imaging to guide surgeons during the resection of tumors. This technique would fully exploit the resolution of ultrasound scanner to deliver fluorescent markers with a precision within 1 mm. These composite droplets and their release with a clinical scanner were tested in chicken embryo.[24–26] Since then, Fabilli *et al.*[21] and Rajian *et al.*[27] have reproduced these composite droplets and inserted thrombin and ICG for *in vitro* release. However, it remains unclear if these composite droplets can circulate freely in a mature vasculature and if they can extravasate their content within mammal tissue.

This study is the first demonstration that a large amount of an encapsulated agent can be released *in vivo* in a controlled manner thanks to the high spatial and temporal resolution allowed by an ultrasound scanner. Fluorescein, a marker easily observable within tissue, is used here to illustrate the local delivery of large payloads. The paper describes the preparation and injection method of the composite emulsion, its ultrasound release in the liver and its monitoring by acoustic and fluorescent means. Such demonstration opens new perspectives for efficient drug delivery performed and guided with a single clinical scanner.

II. METHOD

II.A. Composite droplet preparation and characterization

Production of the droplets was described in the initial paper and patent.[24–26] The first step is the formation of a primary emulsion (peak = 230 nm, standard deviation = 100 nm), which is then injected within a microfluidic channel to yield 4 μm composite droplets. As compared to the previous study, the surfactant was modified to improve the purity of the ammonium salt derived from Krytox [Fig. 1(a)]. This step improves stability of the droplets and fluorescein is conserved within the droplets for up to 21 days. The fluorescein content of the inner aqueous phase was saturated to 0.3 g/l, which is beyond the threshold for fluorescence quenching. The droplets were concentrated by centrifugation to a concentration of 500×10^6 droplets per ml and then refrigerated until the injection within the femoral vein of the rats.

II.B. Animal preparation

All experiments were carried out in accordance with the European Communities Council Directive of November 24

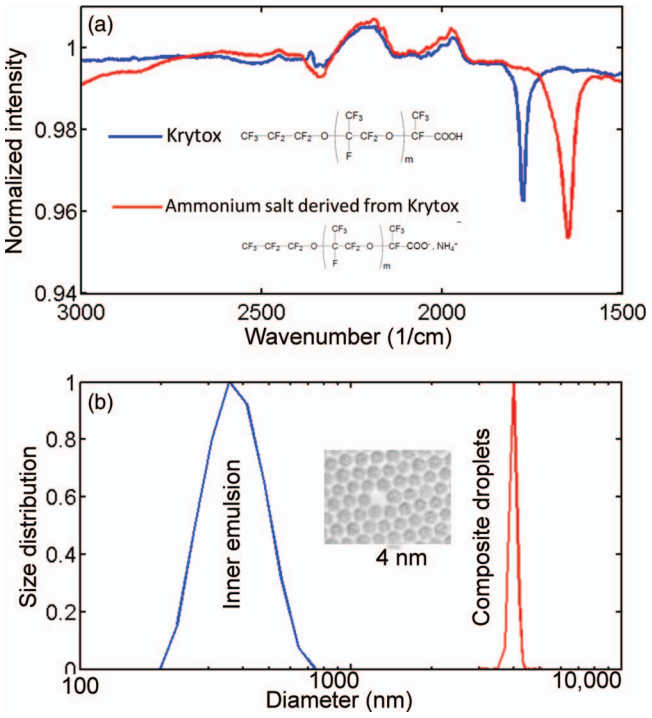

FIG. 1. (a) Infrared spectra of the surfactant after reaction of Krytox with ammonium salt. With the new, nonhydrated, single-step synthesis, a single peak of pure modified-Krytox is obtained. (b) Microscopy of droplets and resulting distribution of the sizes. The nanoemulsion is 230 nm in diameter and the composite droplets are monodisperse at 4 μm diameter.

1986 (86/609/EEC). A total of 12 male Sprague–Dawley rats weighing between 120 and 200 g were used, after having been kept on a 12-h dark/light cycle at a temperature of 22 °C with food and water available *ad libitum*. Prior to surgery, animals were anesthetized with urethane (1.25 g/kg ip) with additional doses (0.1 ml) administered if required. The animals were laid down in supine position on a homeothermic blanket (Braintree Scientific) to maintain body temperature at 37 °C throughout surgical and experimental procedures. For each animal, the fur on the rat abdomen around the scanning site was removed with a depilatory cream. An aqueous ultrasound gel pad (Aquaflex) was used to apply ultrasound. For intravenous injection of composite droplets, the right femoral vein was cannulated with polyethylene tubing connected to a 1 ml syringe and 100 μl of 1% sodium citrate was administered intravenously as an anticoagulant. One minute before the first ultrasound release, 100 μl of composite droplets (total of 50×10^6 droplets) and 50 μl sulforhodamine B (5 mg/ml) (Sigma-Aldrich) were injected before being flushed by 100 μl of saline.

II.C. Ultrasound imaging and release

Before injection, a 5 MHz transducer array (128 elements, 0.3 mm pitch) was aligned in the axial plane over the liver as shown in Fig. 2. The array was connected to an ultrafast ultrasound scanner [Aixplorer, Supersonic Imagine, Aix-en-Provence, France] capable of transmitting and receiving any dedicated ultrasound sequence on 128-independent channels.

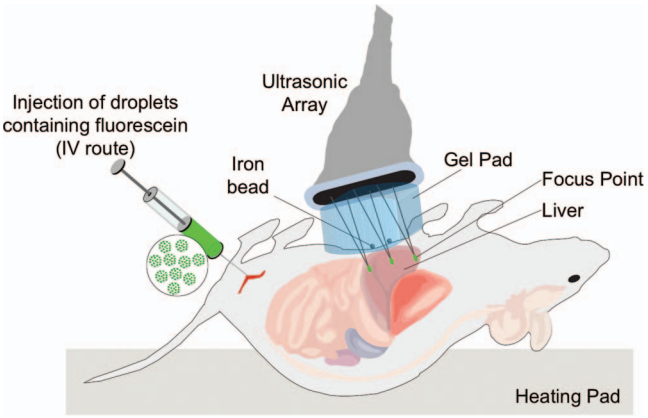

FIG. 2. Setup for the injection and ultrasound-induced release in the liver. The rat is anesthesized and placed over a heating pad before the composite droplets are injected in a femoral catheter. The ultrasound array is used to image and identify the region of interest in the liver and to focus short ultrasound pulses to convert the droplet and release the fluorescein. The liver is then exposed and observed under a macroscope.

Customized emission patterns were programmed on homemade MATLAB dynamic link libraries (Mathwork) driving the ultrasonic scanner. At first, a conventional B-mode image was obtained and displayed so that the user could pinpoint five target zones of release in the liver. An M-Mode was then obtained for respiratory gating.

The release sequence itself was composed of a set of plane wave transmissions for ultrafast imaging,[23,28] followed by focused pulses at five different depths (axial = 16, 18, 20, 22, and 24 mm) on each of the five target zones. The five target zones were submitted to different peak-negative pressures [1.2, 2.0, 2.6, 3.5, and 4.4 MPa-peak-negative pressure (PNP) nonderated] to determine the *in vivo* threshold of release. All pulses were separated by, at least, 150 μs and were five cycles in length (maximal duty cycle = 0.1% but generally closer to 0.03% at each point), depending on the number of imaging plane waves required. This sequence was then repeated 1000 times with respiratory gating. Another set of sequences varied the number of pulses focused at each point, from 1 to 30 000 pulses at specific peak-negative pressures (3.5, 4.0, and 4.4 MPa PNP).

A final conventional B-mode image was obtained for comparison. The echoes obtained for all these pulses, in particular from the ultrafast plane wave, were imported and beamformed to produce ultrasound movies of the release at 260 Hz frame rate. These movies were then filtered to remove slow moving tissue, in a process similar to micro-Doppler.[29–31]

The localization and release were confirmed throughout the experiment with higher quality ultrasound images obtained from the clinical software running on a second Aixplorer scanner using an 8 MHz linear array.

II.D. Macroscopy

Immediately after ultrasound imaging and release, a 5-cm midline laparotomy was performed to assess the external effects of droplet's release. Pictures of the liver were taken at

a 1.25× magnification using a MZ10F fluorescence stereomicroscope (Leica Microsystems) equipped with both GFP Plant (Exc:470/40 nm, Em:525/50) and ET DsRed (Exc:545/30, Em:620/60) filter sets (Leica Microsystems) and interfaced to a Retiga-SRV CCD camera (Q-imaging).

II.E. Intraoperative fluorescent imaging

The exposed liver was also imaged with a FluobeamTM 500 (Fluoptics, Grenoble France), an intraoperative fluorescent camera highly sensitive to fluorescein. Images were recorded in real time, after injection and ultrasound release, to guide manipulation.

II.F. Histopathological studies of rat livers

Quickly after observation under the macroscope, animals were sacrificed by cervical dislocation and livers samples of both labeled and unlabeled regions were isolated using sterile instruments, immersed in a beaker of isopentane cooled to −40 °C in a dry ice bath and frozen for 5 min. The frozen tissue was wrapped in parafilm, placed in a sealed watertight container and store at −80 °C. Prior to slicing, the fresh frozen tissue was transferred from storage to the cryostat, allowing the tissue to slowly equilibrate to the chamber temperature of −20°C for 30 min. Livers were then processed into 40 μm thick sections using a cryostat (Leica Instruments). To evaluate safety and efficacy of droplet release, the samples were collected with or without staining with hematoxylin-eosin mounted with organolemon mounting medium (Invitrogen) and observed under fluorescence microscope (ZEISS, Imager M1) or confocal microscope (Nikon A1, Nikon).

III. RESULTS

III.A. Ultrasound imaging, release, and monitoring

Exploratory imaging was performed with the 8 MHz probe in B-mode (conventional view), color Doppler and elasticity imaging modes. The liver of the rat extended from below the ribs and the sternum, where it covered most of the cross section of the rat, to about 1 cm posterior to the sternum (ventral) where it progressively yielded to the intestine. The motion amplitude of the liver due to breathing appeared to be 5 mm and was measured with an M-mode (repeated single-line view) to about 2 Hz.

After the intravenous injection of the droplets, the sonographer was shown an image obtained with the 5 MHz array and selected the five target zones on the screen with a pointer. A single release sequence lasted less than 1 s, which included the transfer of all the echo data recorded after focused pulses and plane-wave imaging. For large number of pulses, this sequence was repeated ten times (Fig. 2).

At first, B-mode images were compared before and after the release [Figs. 3(a) and 3(b)]. The liver was seen as a uniform mass below the skin (hyperechoic surface). The image

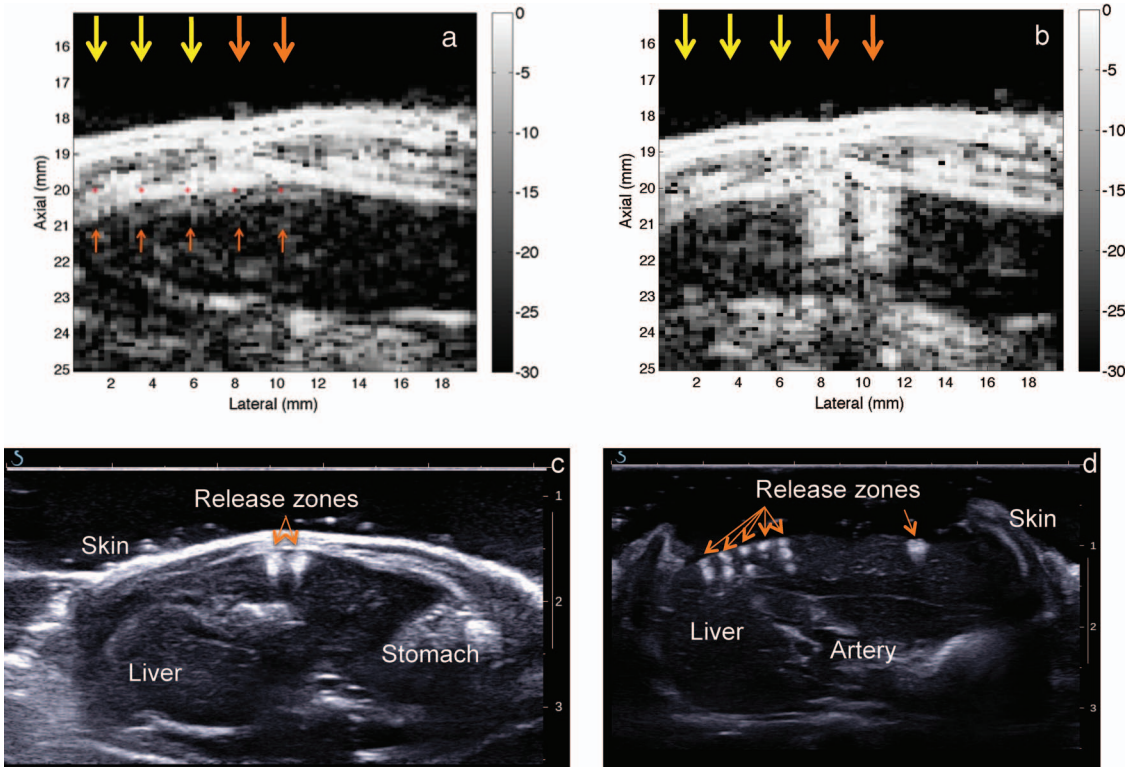

FIG. 3. (a) Conventional 5 MHz B-mode of the liver in the region of interest prior to the ultrasound-induced release. The arrows point at the five focal release zones selected by the user directly on the image (from left to right: 1.2 MPa, 2 MPa, 2.6 MPa, 3.5 MPa, and 4.4 MPa peak-negative pressure). (b) Conventional B-mode of the liver after the ultrasound-induced release. In average, the two zones are 25 dB more echoic with respect to the early image. (c) B-scan over a wider region of the liver with a 8 MHz transducer after the two-points ultrasound-induced release. (d) B-scan of an exposed liver over a five-points release (left of the liver) and a two-points release (right).

obtained at the end of the experiment showed clearly two hyperechoic regions, 25 dB brighter than the surrounding tissue. These regions corresponded to the 3.5 and 4.4 MPa peak-negative pressure, while the lower pressures (1.2, 2.0, and 2.6 MPa) did not induce the formation of such artifacts. The hyperechoic spots were well separated by 2.25 mm as defined by the user. Their width was less than 1.5 mm, while their depth range was closer to 2 mm.

Throughout the experiment, plane-wave ultrafast imaging was performed between release pulses.[24,28] The 260 Hz ultrasound movie obtained within the sequence could thus be exploited to follow the apparition of the hyperechoic spots. As in ultrafast Doppler signal processing,[30,29,31] slow moving tissue could be easily filtered out from a large set of images. Rapid changes could be detected specifically in the regions corresponding to the 3.5 and 4.4 MPa target site [Fig. 4(a)]. Disregarding the artifact due to the filter, it could be seen that such echo variation appeared just after the first few release pulses and continued at the same rate throughout the sequence [Fig. 4(b)]. Such decorrelation intensity could be measured at the release site and reached up to 20 dB over the baseline decorrelation within tissue. The two regions observed on B-mode imaging acquired their specific appearance well within 10 ms, as compared to other spots insonified below apparent threshold level.

Figure 4(c) shows another set of experiments where five series of 4.4 MPa PNP pulses were focused at different points for varying duration. A single pulse decorrelated the tissue echo by 10 dB for less than 1 ms, while longer series of pulses decorrelated the signal for the entire duration of the sequence. At the end of the release sequence, the decorrelation diminished to the background level. Thus, the hyperechoic regions remained, but their rapid variation stopped.

The hyperechoics regions on the B-mode and ultrafast decorrelation images were used as feedback by the sonographer to determine the success of the release. Indeed, these two phenomena were correlated in a former study.[24] Such feedback was never observed when the release sequence was performed before the injection of the composite droplets.

In the liver, the hyperechoic regions were observed when the release sequence was applied from 1 to 60 min postinjection [Figs. 3(c) and 3(d)]. The evolution of the hyperechoic region as observed by the 8 MHz array was slow. The target spots were still observed until the termination of the experiment, two hours after the release sequence.

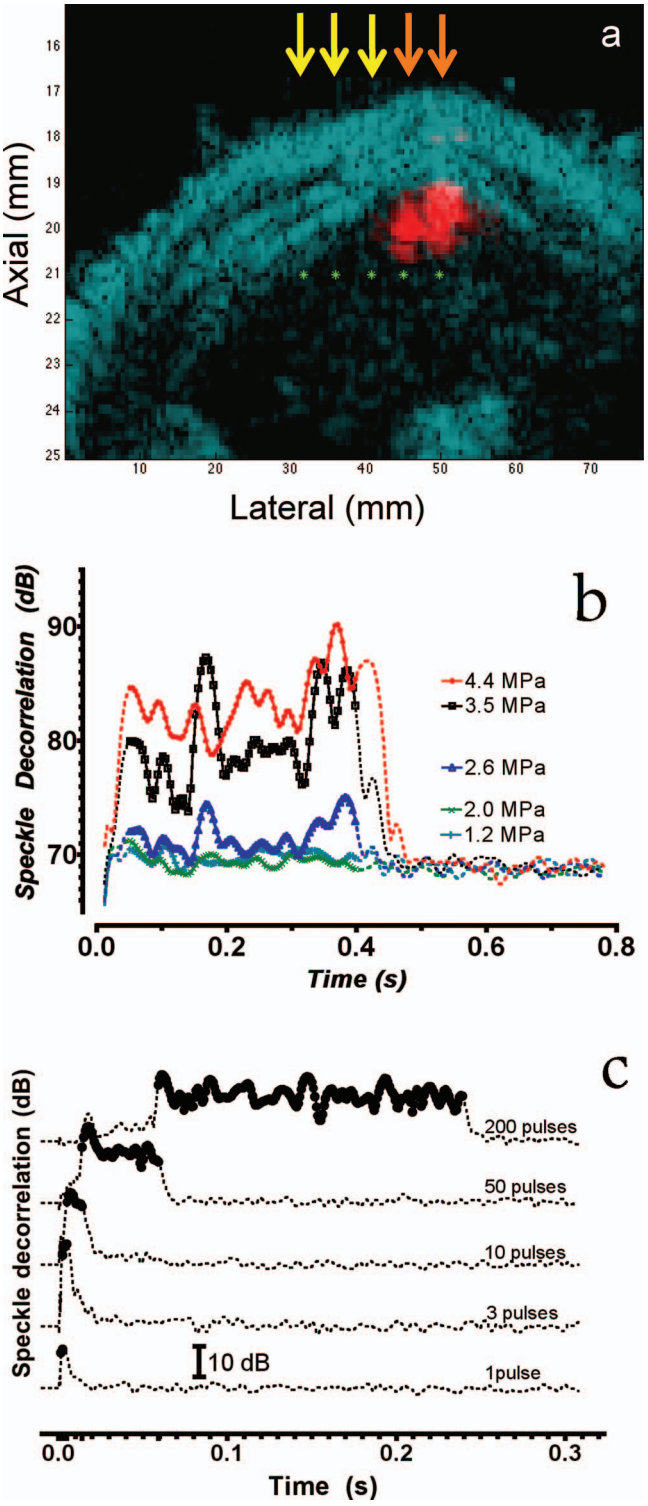

FIG. 4. Ultrasound imaging using plane waves at 1.1 kHz frame-rate. (a) Image of the speckle decorrelation over 300 μs after the start of the release sequence (bright spots) superimposed on the early B-scan (darker background). (b) Tissue Doppler averaged over each regions observed on plane wave imaging with respect to the amplitude of the 1000 focused pulses used for release. (c) Same tissue Doppler for varying number of pulses.

III.B. Macroscopy

After noninvasive release and monitoring of the droplets using the ultrasound clinical scanner, a laparotomy was performed to assess the effects of the release on the liver. A careful inspection was made with a macroscope at three different wavelengths within 15 min of the release sequence. Bright-field images with white-light illumination (Fig. 5, left panel) revealed small black-spotted area with a spatial distribution similar to the hyperechoic regions seen in the ultrasound images. These regions corresponded to the target regions defined by the sonographer. Regions that were insonified with pulse energy below the threshold did not appear fluorescent. At least 35 fluorescent and 12 nonfluorescent subthreshold zones were observed on 5 different rats.

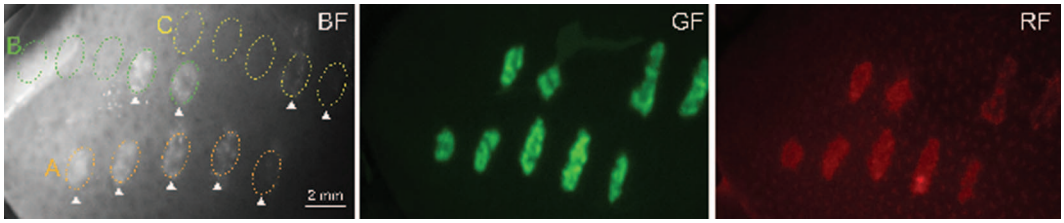

FIG. 5. Macroscopic images of the region showing various parameters of release (left: bright field, center: GFP filter, right: DSred filter). In region A, the five release points were produced with 1, 3, 10, 20, 100 pulses at 4.4 MPa. The two other series B and C were produced with 1000 pulses at 1.2, 2.0, 2.6, 3.5, and 4.4 MPa. Focusing pulses at 1.2, 2.0, and 2.6 MPa did not produce fluorescent regions, nor ultrasound contrast.

The smallest spot, obtained with only 1 pulse at 4.4 MPa PNP, was 1.5 mm × 1 mm in size at the surface. Due to breathing motion, the longer release sequences yield longer spots that were still less than 1 mm wide, but up to 3 mm in length.

The green fluorescence was only transiently present in the release region. It eventually faded 20 min after the release in surviving rats. The fluorescence was conserved when blood circulation was stopped.

On bright field images, the fluorescent zones displayed a higher diffuse scattering as compared to surrounding tissue. When the dsRed filter was used to image sulfurodhamine, the release zones were also contrasting with background tissue. These red fluorescent spots increased in intensity within the first 20 min while the green fluorescence was fading. For 1000 pulses of 5 cycles (PRF = 260 Hz) repeated at a single site, release of fluorescein along with hyperechoic regions in ultrasound images was observed for pulses over 2.6 MPa PNP at 5 MHz (mechanical index, MI = 1.2). For a single pulse, only the highest pressure released the droplets (4.4 MPa, MI = 2.0).

III.C. Intraoperative fluorescent imaging

In Fig. 6, the intraoperative Fluobeam was used to observe the green fluorescent dots on the liver of the rat. Apart from these regions of release, the liver appeared uniformly dark as compared to skin and intestines. The three zones of release on this rat were seen on both sides of the right lobe. Fluorescent zones were also observed in the caudate lobe in corresponding zones.

III.D. Microscopy

Liver samples were obtained after the injection of the droplets, but without exposure to ultrasound (Fig. 7). Even several weeks after fixation, the droplets were observed within the vasculature and they retained their grape-like appearance and 4 μm diameter.

H&E staining was also performed on slices of tissue that were submitted or not to ultrasound release pulses (Fig. 8). The tissue structure appeared to be preserved at the site of the release of the fluorescein and cells remained intact over slices.

IV. DISCUSSION

The goal of this study was to perform controlled release of large amounts of a hydrophilic agent (fluorescein) in rat's liver with a millimetric resolution using an ultrasound scanner and composite droplets injected intravenously. The first step was to describe the ultrasound focusing sequence and the resulting acoustic contrast. The second step was to demonstrate the strong fluorescent signal resulting from the ultrasound-induced release of fluorescein in specific zones of the liver.

The production of the droplets was described in earlier publications.[24–26] They were previously shown to be sensitive

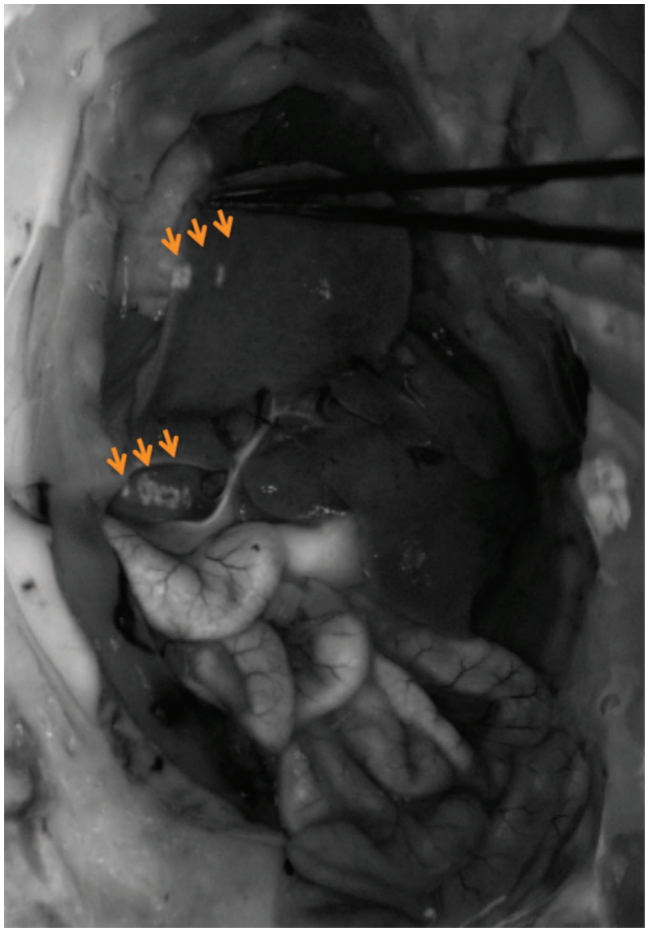

FIG. 6. Intraoperative fluorescent imaging of the liver after the release of the droplets in the right lobe of the liver of a rat. Holding the lobe exposes the effect of the release on the lower lobe directly underneath.

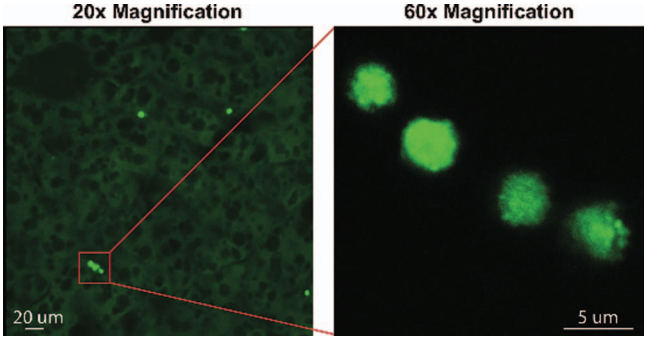

FIG. 7. Microscopy of liver tissue after the injection of composite droplets. Their semiquenched fluorescence, distinct grainy appearance and size allow them to be recognized within the vasculature.

to ultrasound pulses that can be generated by commercial ultrasound imaging scanners. Due to the large fluorescent payload within the carrier, the released fluorescein was sufficiently bright to be observed with a simple set of orange goggles and blue illumination. These results encouraged our group to attempt tattooing mammal tissue *in vivo*.

The experiments with optimal parameters were performed on five rats. However, the droplets were injected intravenously in 12 rats at the minimal dose of 50×10^6 droplets. No obvious side effects of the injection were observed as the animals were handled for 2 h before sacrifice. Even after several days of fixation of the liver, the droplets retain their grape-like appearance under fluorescent imaging. Microscopy and ultrasound monitoring outside the release region suggests that the droplets are rapidly eliminated from the brain and accumulate within the blood vessels of the liver. Such behavior resembles that of sonazoid, an ultrasound contrast agent, used for its specific ability to accumulate within the Kupffer cells.[32] For liver tattooing, this property increases the number of droplets that can be released. However, modifications of the shell material, such as replacing the poloxamer (Krytox surfactant) by

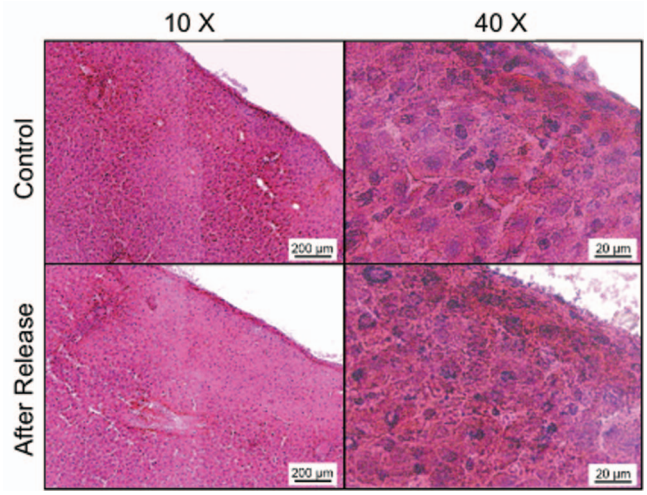

FIG. 8. H&E staining of liver slice that were exposed (after release) or not (control) to ultrasound. The tissue and cellular structure do not appear to be affected by the conversion of the droplets within the vasculature.

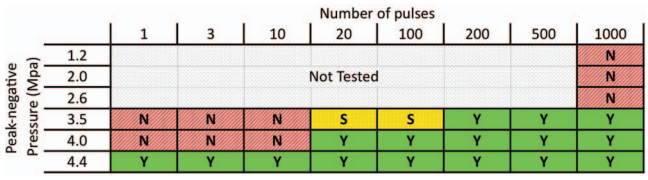

FIG. 9. Summary of the ultrasound parameters required to convert the composite droplets to produce a zone contrasting surrounding tissue both with ultrasound and fluorescent imaging. (Y: Yes, N: No, S: Sometimes). At least 35 distinct release zones were obtained on five different rats.

a polyethylene glycol, are envisioned if accumulation in the liver is detrimental to other applications.

One of the main objectives of this study was to demonstrate that the content of the droplet could be released and monitored with a conventional ultrasound imaging scanner. Figure 9 summarize the conditions for the release of the fluorescein from composite droplets *in vivo*. As imaging arrays and electronic systems are not designed to emit pressures at therapeutic level, the pulses were naturally restricted to 4.4 MPa peak-negative pressure at 5 MHz, which yield a mechanical index of MI = 2. However, release was observed even at lower mechanical index, such as MI = 1.6. Moreover, considering the low duty cycle (less than 0.1%) and the low intensity of a maximum of ISPTA = 220 mW/cm^2, temperature increases should be below 1 °C for liver tissue. Such levels are well within government regulations for an imaging scanner (maximum MI = 1.9, TI = 1). Consequently, the ultrasound conversion of the droplet can be performed with a clinical scanner at levels that should not affect tissue in the absence of droplets. Since all scanners are designed to focus anywhere within the image, this ultrasound-induced drug release would be applicable at any hospital equipped with an ultrasound system. When thinking of applications, it should be considered that the release of the droplets *in vivo* would be strongly affected by the pressure and acoustic frequency at the focus, which are themselve dependent on the depth, attenuation, aperture, and nonlinear acoustic effects. As in ultrasound imaging, lower frequencies should favor penetration, but should also increase the size of the focal spot, worsening the resolution of the technique. Yet, many organs are currently imaged with 5 MHz ultrasound probes and should be considered as primary targets for the release of composite droplets.

The limited intensity levels and temperature increase induced by the ultrasound array also indicate that the conversion of the droplets is not a thermal process. *In vitro* experiments (not shown) demonstrated that longer pulses did not increase the probability of conversion of the droplets. Moreover, higher frequencies were less efficient in releasing the content of the composite agents, while it was still attainable at 8 MHz. Consequently, the process of release of the droplets is likely linked to the pressure change at the focus. In our view, such pressure-induced process is beneficial since pressure is easier to localize as compared to heat.

The ultrasound scanner used for the ultrasound release was also exploited for the controlled monitoring of the release process. Comparing the conventional B-mode made before and

after the release clearly displays two bright (+25 dB) hyperechoic regions corresponding to the zones where higher pressure pulses were focused. From these simple images, the release threshold could be established to between 2.6 and 3.5 MPa PNP as it was later confirmed with the presence of fluorescent spots on the liver. Indeed, the presence of these hyperechoic regions is systematically predictive of the presence of optical contrast. As it was shown with ultrafast monitoring, these bright zones appear with the first release pulse and are observable within 1 ms. Filtering such signal from stationary tissue allows the effect of the release pulse to be monitored. Consequently, tissue damage could be reduced by stopping the sequence as soon as hyperechoic regions are observed. The fact that these hyperechoic regions can last several hours could also be a useful tool to find the region of interest with ultrasound after the operation.

Such hyperechoic regions are commonly observed when a gaseous contrast agent is generated *in vivo* from liquid submicrometer droplets, a process called acoustic droplet vaporization. This mechanism has already been described[20] as a potential contrast agent. These studies have also shown that the liquid droplets can expand sevenfold when converted to gas. These expanded pockets of gas can even be used for tissue occlusion.[33] Contrarily to these former studies, however, the present composite droplets are micrometer-sized. Moreover, they contain a complex emulsion of water within the matrix made of gas-precursor perfluorocarbon. The volume of gas that can be produced during the vaporization of the perfluorocarbon can thus fill the capillaries and create a highly scattering region with ultrasound imaging. For such contrast to last several hours would require the gas to be stabilized, since the boiling point of perfluorohexane (56 °C) is much higher than the body temperature of the rat (38 °C).

The release sites defined by the sonographer and revealed as hyperechoic regions during liver imaging, were shown to be brightly fluorescent. These regions were easily observable with a macroscope, with simple filter goggles and with an intraoperative camera. As stated before, they corresponded systematically to the feedback on the ultrasound images. The fluorescent dots could be less than 1 mm in size, but they were elongated by the tissue motion during the release sequence. These zones were also seen with the Fluobeam, a type of camera currently used for fluorescence imaging in surgery rooms. The release process is observed in several lobes of the liver within the path of the ultrasound beam. The images were used to guide the resection of the liver tissue for fixation, demonstrating at the same time that ultrasound-induced internal tattooing could be used to guide the surgeon toward regions that would be otherwise difficult to identify.

The fluorescent dots faded after 15 min when the rats were alive, which might be due to the fast diffusion of the small molecules of fluorescein (332 Da) toward circulation. Larger fluorescent markers could potentially be used to extend the life of the internal tattoo. Interestingly, ultrasound contrast was more persistent than fluorescent dots, which seems to suggest that, while bubbles remain trapped, small molecules can leak within tissue. The red fluorescence of sulfurhodamine increased with time following the release sequence. After 1 h, most of the green fluorescence was eliminated, leaving only bright red dots which highlighted extravasation induced by the conversion of the droplets.

When the number of release pulses was kept below 1000 pulses, minimal effects were seen at the surface of tissue. Microscopy of these zones after fixation did not show clear damage to the vascular network or toward cells. Since this study was a proof of concept of the release of large payloads with an ultrasound scanner, tissue damage and biocompatibility of the droplets was not studied in a great extent. Future endeavors would be concerned with long-term viability of the rats after injection and induced release. As mentioned before, the shell of the droplets could be modified to increase the circulation time of the droplets. It would also be necessary to describe the physical process of the release and the accompanying extravasation of the agent.

Fluorescein was used as an illustration for the encapsulation of a clinical agent within the composite droplets and its release *in vivo*. This ultrasound-induced local fluorescence could be applied for the internal tattooing of tissue *in situ*, as described initially.[24–26] Following our early description of these double-emulsions, the group of the University of Michigan (Refs. 21 and 27) has described the encapsulation of other molecules such as indocyanine green for photoacoustic imaging and thrombin for embolization. Although these experiments were performed *in vitro*, they demonstrate that a wide variety of molecules could be released by an ultrasound clinical scanner *in situ*. For instance, other applications can be envisioned such as the release of chemotherapeutic drugs to preserve tissue outside of the focal zone defined by the sonographer. Since we observed no damage to the surrounding tissue in the liver, we can also imagine using these droplets for gene transfection.

V. CONCLUSION

This study demonstrated that composite nanodroplets could carry large payloads of a hydrophilic compound and release it *in vivo* to a targeted region in a safe and controlled manner. In this particular case, fluorescein was released *in situ* in the rat liver to create a genuine internal tattoo from a virtual drawing within the ultrasonic image. Such a process could help radiologists to guide surgeons prior to surgery. These droplets can be converted by focused pulses generated by a clinical ultrasound scanner at pressures which are below regulations for medical imaging. In parallel, the same ultrasound array can monitor the process since strongly hyperechoic regions accompany the release of the droplets. Since no modification of the hydrophilic agents is necessary to be encapsulated in composite droplets, various other drugs could be release *in situ*.

ACKNOWLEDGMENTS

We thank Damien Belotti and Janine Cossy for their essential help in stabilizing the composite droplets. We thank

Pierre-Alix Dancer and Fluoptics for providing and handling the Fluobeam intraoperative camera.

[a]Author to whom correspondence should be addressed. Electronic mail: olivier.couture@espci.fr; Telephone: (+33) 6 50 87 08 96.
[b]These authors contributed equally to this publication.

[1]G. ter Haar, "Therapeutic applications of ultrasound," Prog. Biophys. Mol. Biol. **93**(1–3), 111–129 (2007).
[2]F. Marquet, M. Pernot, J.-F. Aubry, G. Montaldo, M. Tanter, and M. Fink, "Non-invasive transcranial ultrasound therapy guided by CT-scans," in *Proceedings of the Annual International Conference of the IEEE Engineering in Medicine and Biology Society* (IEEE, New York, 2006), Vol. 1, pp. 683–687.
[3]T. Hall, J. Fowlkes, and C. Cain, "A real-time measure of cavitation induced tissue disruption by ultrasound imaging backscatter reduction," IEEE Trans. Ultrason. Ferroelectr. Freq. Control **54**(3), 569–575 (2007).
[4]H. Maeda *et al.*, "Targeted drug delivery system for oral cancer therapy using sonoporation," J. Oral Pathol. Med. **38**(7), 572–579 (2009).
[5]A. Mesiwala *et al.*, "High-intensity focused ultrasound selectively disrupts the blood-brain barrier *in vivo*," Ultrasound Med. Biol. **28**(3), 389–400 (2002).
[6]C. Caskey, X. Hu, and K. Ferrara, "Leveraging the power of ultrasound for therapeutic design and optimization," J. Controlled Release **156**(3), 297–306 (2011).
[7]M. Böhmer, A. Klibanov, K. Tiemann, C. Hall, H. Gruell, and O. Steinbach, "Ultrasound triggered image-guided drug delivery," Eur. J. Radiol. **70**(2), 242–253 (2009).
[8]P. Burns and S. Wilson, "Microbubble contrast for radiological imaging: 1. Principles," Ultrasound Q **22**(1), 5–13 (2006).
[9]K. Hynynen, N. McDannold, N. Vykhodtseva, and F. Jolesz, "Non-invasive opening of BBB by focused ultrasound," Acta Neurochir. Suppl. (Wien) **86**, 555–558 (2003).
[10]C.-D. Ohl *et al.*, "Sonoporation from jetting cavitation bubbles," Biophys. J. **91**(11), 4285–4295 (2006).
[11]A. van Wamel *et al.*, "Vibrating microbubbles poking individual cells: Drug transfer into cells via sonoporation," J. Controlled Release **112**(2), 149–155 (2006).
[12]B. Meijering *et al.*, "Ultrasound and microbubble-targeted delivery of macromolecules is regulated by induction of endocytosis and pore formation," Circ. Res. **104**(5), 679–687 (2009).
[13]S. Tinkov, R. Bekeredjian, G. Winter, and C. Coester, "Microbubbles as ultrasound triggered drug carriers," J. Pharm. Sci. **98**(6), 1935–1961 (2009).
[14]M. Cochran, J. Eisenbrey, R. Ouma, M. Soulen, and M. Wheatley, "Doxorubicin and paclitaxel loaded microbubbles for ultrasound triggered drug delivery," Int. J. Pharm. **414**(1–2), 161–170 (2011).
[15]B. Geers, I. Lentacker, N. Sanders, J. Demeester, S. Meairs, and S. De Smedt, "Self-assembled liposome-loaded microbubbles: The missing link for safe and efficient ultrasound triggered drug-delivery," J. Controlled Release **152**(2), 249–256. (2011).
[16]G. Casey *et al.*, "Sonoporation mediated immunogene therapy of solid tumors," Ultrasound Med. Biol. **36**(3), 430–440 (2010).
[17]P. Sheeran, S. Luois, P. Dayton, and T. Matsunaga, "Formulation and acoustic studies of a new phase-shift agent for diagnostic and therapeutic ultrasound," Langmuir **27**(17), 10412–10420 (2011).
[18]N. Reznik, R. Williams, and P. Burns, "Investigation of vaporized submicron perfluorocarbon droplets as an ultrasound contrast agent," Ultrasound Med. Biol. **37**(8), 1271–1279 (2011).
[19]K.-I. Kawabata, N. Sugita, H. Yoshikawa, T. Azuma, and S.-I. Umemura, "Nanoparticles with multiple perfluorocarbons for controllable ultrasonically induced phase shifting," Jpn. J. Appl. Phys. **44**(6B), 4548–4552 (2005).
[20]M. Fabiilli, K. Haworth, N. Fakhri, O. Kripfgans, P. Carson, and J. Fowlkes, "The role of inertial cavitation in acoustic droplet vaporization," IEEE Trans. Ultrason. Ferroelectr. Freq. Control **56**(5), 1006–1017 (2009).
[21]M. Fabiilli, J. Lee, O. Kripfgans, P. Carson, and J. Fowlkes, "Delivery of water-soluble drugs using acoustically triggered perfluorocarbon double emulsions," Pharm. Res. **27**(12), 2753–2765 (2010).
[22]M. Seo, I. Gorelikov, R. Williams, and N. Matsuura, "Microfluidic assembly of monodisperse, nanoparticle-incorporated perfluorocarbon microbubbles for medical imaging and therapy," Langmuir **26**(17), 13855–13860 (2010).
[23]O. Couture, S. Bannouf, G. Montaldo, J.-F. Aubry, M. Fink, and M. Tanter, "Ultrafast imaging of ultrasound contrast agents," Ultrasound Med. Biol. **35**(11), 1908–1916 (2009).
[24]O. Couture *et al.*, "Ultrasound internal tattooing," Med. Phys. **38**(2), 1116–1123 (2011).
[25]O. Couture, N. Pannacci, P. Tabeling, M. Fink, V. Servois, and M. Tanter, "Ultrasound-inducible fluorescent particles for internal tattooing," in *Proceedings of the IEEE UFFC Conference*, Roma, 2009.
[26]O. Couture, N. Pannacci, P. Tabeling, M. Tanter, and M. Fink, France Patent PCT/FR2010/051439 (July 17, 2009).
[27]J. Rajian, M. Fabiilli, J. Fowlkes, P. Carson, and X. Wang, "Drug delivery monitoring by photoacoustic tomography with an ICG encapsulated double emulsion," Opt. Exp. **19**(15), 14335–14347 (2011).
[28]G. Montaldo, M. Tanter, J. Bercoff, N. Benech, and M. Fink, "Coherent plane-wave compounding for very high frame rate ultrasonography and transient elastography," IEEE Trans. Ultrason. Ferroelectr. Freq. Control **56**(3), 489–506 (2009).
[29]M. Couade *et al.*, "Quantitative assessment of arterial wall biomechanical properties using shear wave imaging," Ultrasound Med. Biol. **36**(10), 1662–1676 (2010).
[30]M. Couade *et al.*, "*In vivo* quantitative mapping of myocardial stiffening and transmural anisotropy during the cardiac cycle," IEEE Trans. Med. Imaging **30**(2), 295–305 (2011).
[31]E. Macé, G. Montaldo, I. Cohen, M. Baulac, M. Fink, and M. Tanter, "Functional ultrasound imaging of the brain," Nat. Methods **8**(8), 662–664 (2011).
[32]K. Yanagisawa, F. Moriyasu, T. Miyahara, M. Yuki, and H. Iijima, "Phagocytosis of ultrasound contrast agent microbubbles by Kupffer cells," Ultrasound Med. Biol. **33**(2), 318–325 (2007).
[33]O. Kripfgans, M. Fabiilli, P. Carson, and J. Fowlkes, "On the acoustic vaporization of micrometer-sized droplets," J. Acoust. Soc. Am. **116**(1), 272–281 (2004).